

# In Vitro Performance of Published Glypican 3-Targeting Peptides TJ12P1 and L5 Indicates Lack of Specificity and Potency

Rose M. Berman,<sup>1</sup> Olivia J. Kelada,<sup>1,2</sup> Nicholas T. Gutsche,<sup>1</sup> Raju Natarajan,<sup>3</sup> Rolf E. Swenson,<sup>3</sup> Ying Fu,<sup>4</sup> Jessica Hong,<sup>4</sup> Mitchell Ho,<sup>4</sup> Peter L. Choyke,<sup>1</sup> and Freddy E. Escorcía<sup>1</sup>

## Abstract

**Background:** Glypican 3 (GPC3), a plasma membrane heparan sulfate proteoglycan, is overexpressed on human hepatocellular carcinoma and may represent a promising biomarker. Several studies have reported peptides that selectively bind to GPC3 and could serve as scaffolds for imaging or therapeutic agents.

**Materials and Methods:** We synthesized variants of two previously published peptides, DHLASLWWGTEL (TJ12P1) and RLNVGGTYFLTTRQ (L5), and evaluated their *in vitro* binding performance in paired isogenic cell lines, A431(GPC3<sup>-</sup>) and A431-GPC3<sup>+</sup> (G1), as well as the liver cancer cell line HepG2. Using flow cytometry and biolayer interferometry (BLI), we compared the binding of the TJ12P1 and L5 peptide variants to the binding of corresponding scrambled peptides having the same amino acid composition, but in random sequence.

**Results:** While both peptides bound to G1 and HepG2, they also bound to A431. The corresponding scrambled peptides demonstrated greater apparent binding to both G1 and A431 than their specific counterparts. BLI confirmed lack of binding at 0.5–1  $\mu$ M for both peptides.

**Conclusions:** We conclude that neither TJ12P1 nor L5 variant demonstrates selectivity for GPC3 at concentrations near the reported  $K_D$ , and that the peptides lack potency or are nonspecific, making them inadequate for use as imaging agents.

**Keywords:** GPC3, hepatocellular carcinoma, peptide

## Introduction

Hepatocellular carcinoma (HCC) represents about 90% of all cases of primary liver cancer, ranking as the sixth most common neoplasm and the third leading cause of cancer death worldwide.<sup>1,2</sup> In contrast to trends of other malignancies in the United States, HCC incidence and mortality are increasing.<sup>3</sup> Diagnosis and surveillance of HCC typically involve ultrasound, computed tomographic, and/or magnetic resonance imaging. Treatment can range from transplant, surgical resection, or local ablative therapies such as radiofrequency ablation, transarterial embolization, or stereotactic

radiotherapy.<sup>4</sup> Systemic agents such as tyrosine kinase inhibitors (e.g., sorafenib and lenvatinib) can be deployed in the more advanced setting.<sup>5,6</sup> Despite several options for interventions, no truly tumor-selective imaging or therapeutic agents exist for clinical use.

Glypican 3 (GPC3) is a plasma membrane heparan sulfate proteoglycan that is both overexpressed in and characteristic of HCC, suggesting it may be a promising tumor-selective biomarker.<sup>7</sup> Several full-length antibodies, antibody fragments, and peptides for imaging and/or therapeutic use have been developed for GPC3 with varying degrees of success (Table 1).<sup>8–17</sup> While full-length antibodies and antibody

<sup>1</sup>Molecular Imaging Program, Radiation Oncology Branch, National Cancer Institute, National Institutes of Health, Bethesda, Maryland.

<sup>2</sup>In Vivo Imaging, Discovery and Analytics, PerkinElmer, Inc., Hopkinton, Massachusetts.

<sup>3</sup>Imaging Probe Development Center, National Heart, Lung and Blood Institute, National Institutes of Health, Bethesda, Maryland.

<sup>4</sup>Laboratory of Molecular Biology, National Cancer Institute, National Institutes of Health, Bethesda, Maryland.

© Rose M. Berman et al. 2019; Published by Mary Ann Liebert, Inc. This Open Access article is distributed under the terms of the Creative Commons License (<http://creativecommons.org/licenses/by/4.0>), which permits unrestricted use, distribution, and reproduction in any medium, provided the original work is properly cited.

Address correspondence to: Freddy E. Escorcía; Molecular Imaging Program, Radiation Oncology Branch, National Cancer Institute, National Institutes of Health; 10 Center Drive, Room 1B55, Bethesda, MD 20892  
E-mail: [freddy.escorcia@nih.gov](mailto:freddy.escorcia@nih.gov)

TABLE 1. A LIST OF PUBLISHED PEPTIDES AND OTHER ANTI-GLYCAN 3-TARGETING MOIETIES

| GPC3-targeting molecule | Humanized | $K_D$ (nM)       | References |
|-------------------------|-----------|------------------|------------|
| DHLASLWWGTEL (TJ12P1)   | N/A       | 390 (with Cy5.5) | 9          |
| RLNVGGTYFLTTRQ (L5)     | N/A       | 44.7             | 7,10       |
| DYEMHLWWGTEL (IPA)      | N/A       | 225.1            | 14         |
| THVSPNQGLPS (GBP)       | N/A       | 753              | 15         |
| hGC33                   | Yes       | 0.67             | 16         |
| YP7 (hYP7)              | Yes       | 0.3 <sup>a</sup> | 12         |
| HN3                     | Yes       | 0.6              | 8          |
| HS20                    | Yes       | 0.3              | 17         |
| $\alpha$ GPC3-F(ab')    | No        | 0.03             | 13         |

<sup>a</sup> $K_D$  value is for the nonhumanized version of the antibody, as no  $K_D$  was reported for the humanized variant (hYP7).  
 GPC3, Glypican 3.  
 N/A, not applicable.

derivatives have demonstrated apparent *in vivo* localization, we were interested in evaluating small molecules to use as imaging scaffolds due to the potential for same-day imaging and, perhaps, improved tumor penetration.<sup>13</sup> Of the published GPC3-selective peptides, they selected DHLASLWWGTEL (TJ12P1) and RLNVGGTYFLTTRQ (L5) due to their comparatively low reported dissociation constants ( $K_D$ ). Zhu et al. reported the  $K_D$  of Cy5.5-TJ12P1 to be  $390.03 \pm 27.47$  nM.<sup>9</sup> Although the original article describing L5 did not report a  $K_D$ , Wang et al. found the  $K_D$  of the unmodified peptide to be 44.7 nM through surface plasmon resonance.<sup>10,11</sup>

In this study, we synthesize unlabeled and sulfo-Cy5-conjugated variants of TJ12P1 and L5 to assess their ability to bind specifically to GPC3 in cell-based and cell-free assays.

Typically, peptides used successfully as molecular imaging agents require  $K_D$  or  $IC_{50}$  values below 20 nM.<sup>18–22</sup> Given that the reported binding affinities of both peptides were much higher than this threshold, our goal was to first confirm their GPC3 binding *in vitro* at concentrations near their reported  $K_D$  values and then alter the peptide sequences to develop higher-affinity, peptide-based imaging probes for HCC and other GPC3-expressing cancers.

## Materials and Methods

### Cell culture

A431, a human epidermoid carcinoma GPC3<sup>−</sup> cell line, and A431-GPC3<sup>+</sup> (G1), a transfected A431 cell line engineered to stably express human GPC3, were both obtained from Dr. M.H. (National Cancer Institute, Bethesda, MD).<sup>12</sup> HepG2 (GPC3<sup>+</sup> liver cancer cell line) was obtained from ATCC (Manassas, VA). All cell lines were cultured in DMEM (Life Technologies, Carlsbad, CA) supplemented with 10% FetaPlex (Gemini Bio-Products, West Sacramento, CA) according to supplier's protocols. All cell lines tested negative for mycoplasma in monthly tests and were used for experiments within 10 passages (HepG2) or 15 passages (A431 and G1).

### Peptide synthesis

The Imaging Probe Development Center (National Heart, Lung, and Blood Institute, Frederick, MD) synthe-

sized fluorescent and non-fluorescent variants of both peptide sequences, DHLASLWWGTEL (TJ12P1) and KKK-RLNVGGTYFLTTRQ (KKK-L5), as well as two scrambled variants, WLSHLGDLTWEA (TJ12P1 scramble) and KKK-YTRFLGTGVNRLTQ (KKK-L5 scramble), as a control and nonspecific binding blocking agents. TJ12P1 was first synthesized with Cy5.5 as the fluorophore, as per Zhu et al., but due to poor solubility in aqueous solution, a sulfo-Cy5-labeled variant was synthesized and used for experiments.<sup>9</sup> The four peptides—TJ12P1, KKK-L5, and their two scrambled variants—were synthesized with and without sulfo-Cy5 (Supplementary Table S1 and Figures S1–S4).

### Flow cytometry

Approximately  $1 \times 10^6$  cells per sample tube were harvested, washed once with ice-cold staining buffer (1% bovine serum albumin in  $1 \times$  phosphate buffered saline [PBS]), and resuspended in 60  $\mu$ L staining buffer. Cells were then distributed into control and experimental vials. Unstained and single-color control samples were made. Experimental samples were stained with PE-conjugated anti-GPC3 antibody (R&D Systems, Minneapolis, MN), PE-conjugated IgG2 isotype control (Biolegend, San Diego, CA), conjugated specific or nonspecific peptide and incubated for 1–2 h on ice in the dark. Data were collected using a BD FACS-Calibur cytometer running BD CellQuest Pro software (v6.0), and results were analyzed with FlowJo (v10.4.2). All experiments represent biological replicates ( $n=3$ ).

### Bi-layer interferometry

Biotinylated human GPC3 protein (Acro Biosystems, Newark, DE) was diluted to 5  $\mu$ g/mL in assay buffer ( $1 \times$  PBS with 0.02% Tween-20) in a 96-well plate and loaded onto streptavidin biosensors (FortéBio, Menlo Park, CA). Each unconjugated peptide was diluted in assay buffer at four concentrations (1000, 500, 250, and 125 nM for TJ12P1; and 500, 250, 125, and 62.5 nM for KKK-L5) and loaded into the 96-well plate in a final volume of 200  $\mu$ L. Specific and nonspecific binding wells were made for each concentration. The plate was run on an Octet Red96 system (FortéBio) and analyzed with FortéBio Octet Data Analysis software (v.11).

## Results

Solubility assays were performed to determine the most compatible solvent for both peptides before *in vitro* evaluation of GPC3 binding, favoring aqueous solvents over cytotoxic organic solvents such as dimethylformamide (DMF) and dimethyl sulfoxide (DMSO). While Zhu et al. indicated that Cy5.5-TJ12P1 was soluble in DMF at the synthesis stage, authors did not report the formulation for *in vivo* studies.<sup>9</sup> We found this peptide (at 0.3 mg/mL) to be insoluble in ddH<sub>2</sub>O (Fig. 1A) and ddH<sub>2</sub>O+20% DMSO (Fig. 1B), as evidenced by the suspension of blue powder debris in solvent. Sonication and vortexing of samples failed to solubilize the Cy5.5-TJ12P1 powder, and the percent of DMSO was not increased due to the potential for biological toxicity.<sup>24</sup> The sulfo-modified variant, sulfo-Cy5-TJ12P1, appeared to be soluble in 0.15 M NH<sub>4</sub>OAc. Han et al. reported that a variant of the L5 peptide with three lysine residues (KKK-L5) had higher solubility in aqueous solution compared to the original L5 peptide, so this KKK-L5 variant was synthesized<sup>23</sup> and sulfo-Cy5-KKK-L5 were both soluble in ddH<sub>2</sub>O at 0.5 mg/mL.

To confirm the expression of GPC3 in GPC3<sup>+</sup> cell lines (G1 and HepG2), we tested cell binding with flow cytometry. The control A431 cells incubated with buffer, PE anti-GPC3 antibody, or PE IgG2 isotype control antibody demonstrated comparable staining, confirming that A431 does not express GPC3 (Fig. 2A). In contrast, HepG2 (Fig. 2B) and G1 (Fig. 2C) showed a rightward shift of the histogram in the PE channel compared to controls, confirming GPC3 expression in these two cell lines. Because G1 is derived from A431, these two lines are otherwise isogenic and serve as ideal positive and negative controls for GPC3 expression, respectively.

We then performed analogous experiments with sulfo-Cy5-TJ12P1 and its scrambled variant (sequence reported above). Results showed no significant difference in binding between G1, HepG2, and A431 cells after incubation with sulfo-Cy5-TJ12P1 at 325 nM (reported  $K_D = 390$  nM) (Fig. 3A; Table 1).<sup>9</sup> Surprisingly, the sulfo-Cy5-TJ12P1 scrambled peptide at the same concentration demonstrated significantly increased binding in all GPC3<sup>+</sup> cell lines compared to the sulfo-Cy5-TJ12P1 peptide ( $p = 0.02$ ) (Fig. 3B). To rule out the possibility that fluorophore modification of TJ12P1 interfered with its ability to specifically bind GPC3, they performed a cell-free, label-free biolayer interferometry (BLI) assay. BLI-derived association and dissociation curves of unlabeled TJ12P1 at various concentrations to immobilized recombinant biotinyl-

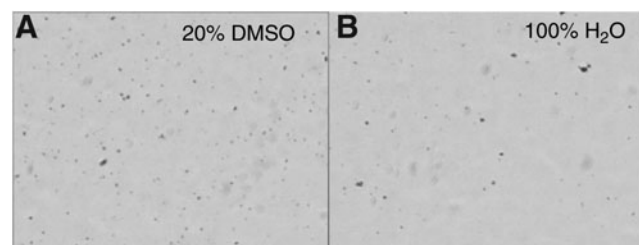


**FIG. 1.** Cy5.5-conjugated TJ12P1 is peptide insoluble in aqueous buffer. Bright field images of Cy5.5-TJ12P1 peptides in solution. In (A, B), peptide Cy5.5-TJ12P1 is undissolved in 20% DMSO/80% ddH<sub>2</sub>O and 100% ddH<sub>2</sub>O at 0.3 mg/mL, respectively. DMSO, dimethyl sulfoxide.

lated GPC3 failed to demonstrate concentration-dependent binding behavior consistent with normal, specific equilibrium binding, and no  $K_D$  could be calculated. In contrast, a known GPC3-specific antibody ( $K_D$  of 4–6 nM) at 150 nM showed  $k_{on}$  and  $k_{off}$  curves consistent with specific binding, and the software was able to confirm the  $K_D$  (Fig. 3C). Although binding curves are somewhat dependent on molecular weight, and TJ12P1 and the positive control molecule differ significantly in this parameter, the association/dissociation curves of TJ12P1 on their own indicate the absence of concentration-dependent binding.

Flow cytometry assays of sulfo-Cy5-KKK-L5 indicate that the peptide bound nonspecifically to GPC3, as the observed histogram shift is identical in the A431 (GPC3<sup>-</sup>) and the HepG2 and G1 (GPC3<sup>+</sup>) cells (Fig. 4A). In addition, the nonspecific peptide (sulfo-Cy5-KKK-L5 scramble) exhibited more binding ( $p < 0.05$ ) than the specific (sulfo-Cy5-KKK-L5) peptide in all three cell lines. The high- and low-staining HepG2 populations both showed statistically significant ( $p < 0.001$  and  $p < 0.005$ ) difference in staining with the nonspecific peptide compared to sulfo-Cy5-KKK-L5 (Fig. 4B). A BLI analysis of the unlabeled KKK-L5 peptide at various concentrations also confirmed absence of specific binding to GPC3 at these concentrations. The nonspecific peptide at the same concentrations performed comparably (Fig. 4C). These results were in contrast to the performance of the known GPC3-specific antibody.

## Discussion

GPC3 is a promising HCC-selective biomarker, and a number of groups have exploited this feature to generate vaccines, HCC-selective antibodies, and peptides for imaging and therapy (Table 1).<sup>25</sup> Several peptides with putative specificity to GPC3 have been reported in the literature. While TJ12P1 and L5 have emerged as the most promising peptides based on published binding affinities, in this study, we demonstrate that neither fluorescently labeled nor unlabeled versions tested can bind to GPC3 at concentrations in the range of their published  $K_D$  (0.3–1  $\mu$ M).<sup>9–11</sup>

Previous studies investigating TJ12P1 and L5 have some limitations, notably absent controls for nonspecific binding on cells,<sup>14</sup> the comparison of nonisogenic cell lines,<sup>26</sup> and the incubation of cells with peptide concentrations well above the reported binding affinities (10–20  $\mu$ M).<sup>10,26</sup> Without using cell lines that only differ in expression of the target of interest to control for off-target associations, or scrambled peptide controls to account for nonspecific peptide-cell interactions, it is difficult to conclude any associations are specific to a target of interest. In the absence of our evaluation of both peptides and their scrambled versions in the A431 cell line (GPC3<sup>-</sup>), to which all peptide variants bound, we may have reasonably concluded that the scrambled peptides were improvements on the originals, as suggested by significantly improved staining of G1(A431-GPC3<sup>+</sup>) and HepG2 cells on flow cytometry. These findings underscore the challenges of peptide engineering and the need for employing multiple assays to corroborate specific binding, as well as appropriate controls to avoid confirmation bias.

The relative hydrophobicity of both peptides may have contributed to their nonspecific binding and makes them

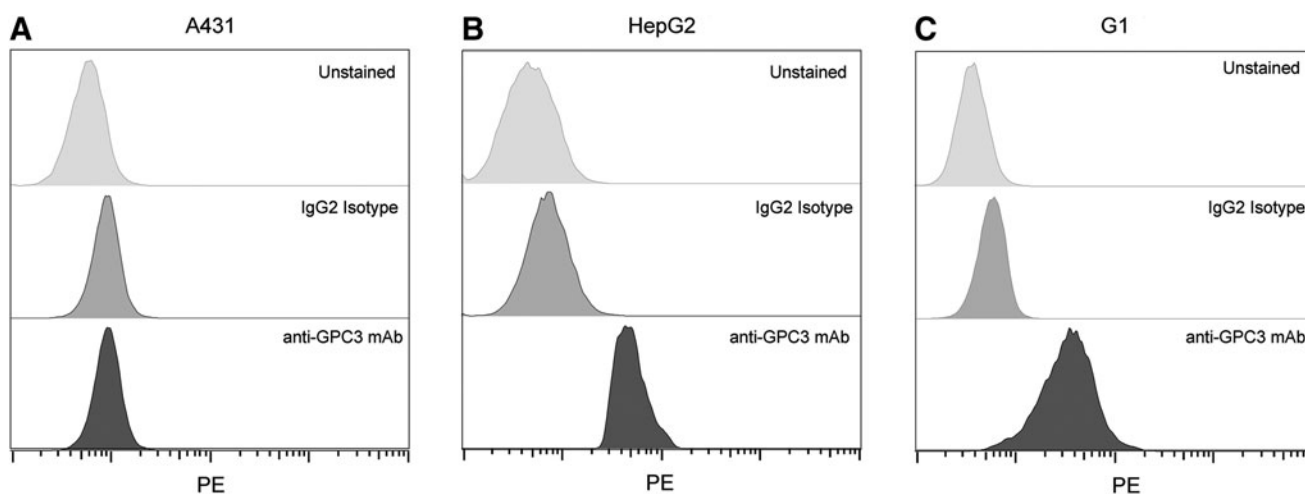


**FIG. 2.** Commercial anti-GPC3 antibody confirms expression of GPC3. Flow cytometry histograms confirming that (A) A431 cell lines do not express GPC3 and that (B) HepG2 and (C) G1 do.

suboptimal translational candidates in their current forms even if they had exhibited potent, specific binding. It is also important to note that the unexpected nonspecific (or nonpotent) binding of TJ12P1 may be explained by the similarity of its sequence to that of peptides found to nonspecifically bind polystyrene walls—a common labware plastic. TJ12P1 was identified by phage panning, a process

that can generate specific peptides as well as “target-unrelated” peptides (TUPs) that bind to components of the screening system such as polystyrene, streptavidin, or bovine serum albumin. Like TJ12P1, many of these TUPs contain two consecutive tryptophan residues.<sup>27</sup> Bakhshinejad et al. suggest depleting the phage library through subtractive biopanning (e.g., by affinity chromatography

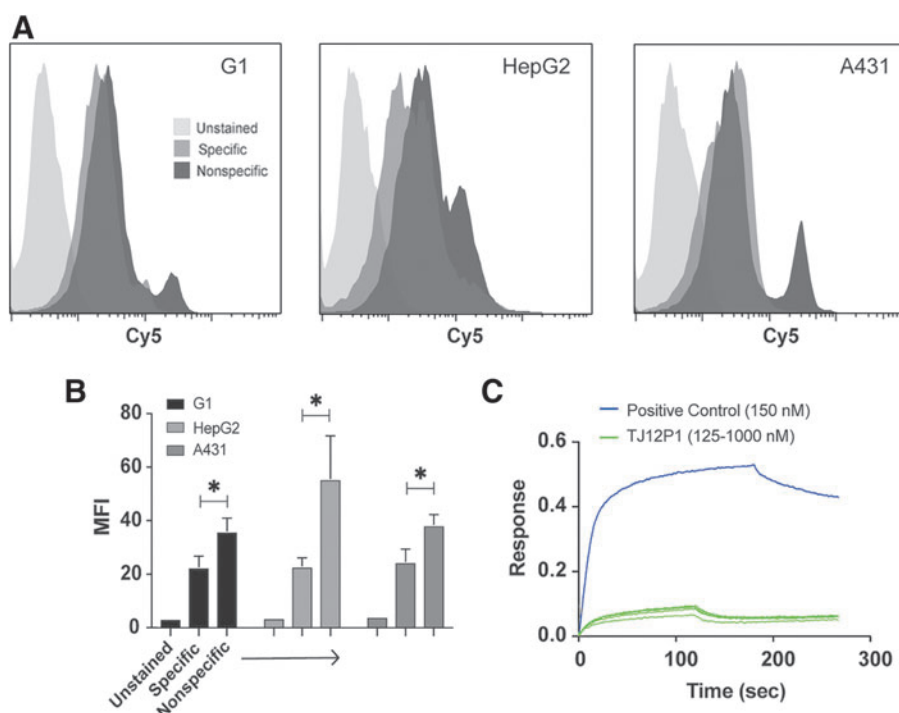


**FIG. 3.** TJ12P1 binds nonspecifically. (A) Flow cytometry histograms of GPC3<sup>+</sup> (G1 and HepG2) and GPC3<sup>-</sup> (A431) cells incubated with 325 nM of sulfo-Cy5-TJ12P1 for 1 h demonstrating nonspecific association of TJ12P1 to all cell lines. (B) Bar graphs of MFI values for all cell lines either unstained or incubated with 325 nM of the specific (sulfo-Cy5-TJ12P1) or nonspecific (TJ12P1 scramble) for 1 h indicating that nonspecific peptide had more binding to all cell lines tested ( $p < 0.05$ ). (C) Bi-layer interferometry response curve shows the association and dissociation of TJ12P1 peptide to recombinant GPC3 at various concentrations (125–1000 nM) compared to a known GPC3-specific molecule ( $K_D$  of 4–6 nM) at 150 nM. TJ12P1 failed to demonstrate concentration-dependent binding behavior consistent with normal, specific equilibrium binding, and no  $K_D$  could be calculated. MFI, mean fluorescence intensity. \* indicates  $p < 0.05$ .

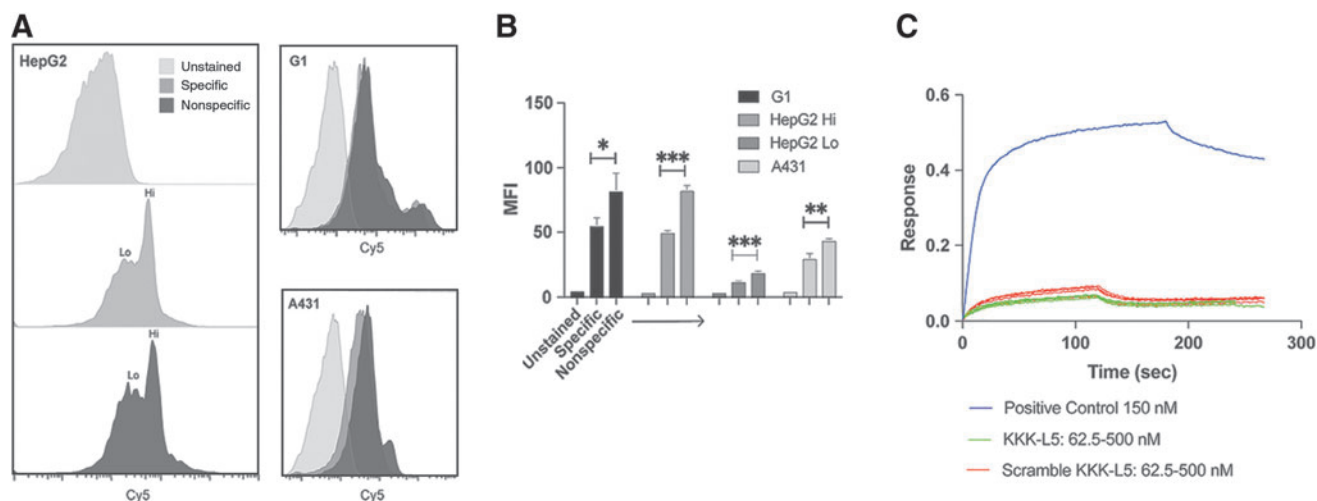


**FIG. 4.** L5 variant binds nonspecifically. (A) Flow cytometry histograms show the Cy5 emission shift in GPC3<sup>+</sup> HepG2 (Lo and Hi were used to differentiate the two HepG2 cell populations with different extent of peptide association) and G1 cells compared to GPC3<sup>-</sup> A431 cells. (B) Bar graph shows MFI values for all cell lines either unstained or incubated with 300 nM of the specific (sulfo-Cy5-KKK-L5) or nonspecific (sulfo-Cy5-KKK-L5 scramble) for 1 h. MFI values suggest that the nonspecific peptide binds better to all cell lines than the specific peptide. \**p* < 0.05, \*\**p* < 0.005, \*\*\**p* < 0.0001. (C) Bi-layer interferometry response curve shows the association and dissociation of KKK-L5 and KKK-L5 scramble to recombinant human GPC3 at various concentrations (62.5–500 nM) compared to a known GPC3-specific molecule (*K<sub>D</sub>* of 4–6 nM) at 150 nM. KKK-L5 failed to demonstrate concentration-dependent binding behavior consistent with normal, specific equilibrium binding, and no *K<sub>D</sub>* could be calculated.

or screening against other cell types) to reduce selection of TUPs.<sup>27</sup> Isogenic cell-based assays could also prove valuable.

In contrast to TJ12P1, L5 was identified by a pull-down immunoprecipitation assay and matrix-assisted laser desorption/ionization-time-of-flight mass spectrometry analysis.<sup>10</sup> Four out of the 14 residues are hydrophobic (28.5%), the presence of which may have contributed to the nonspecific binding of L5 during the selection process.

This study has a few limitations. First, as we were focused on identifying peptides useful at concentrations appropriate for imaging (*K<sub>D</sub>* < 20 nM), we did not test either peptide at concentrations in the high micromolar range, unlike several authors of prior publications. Although one can conclude that TJ12P1 and KKK-L5 do not bind specifically at concentrations in the range of their reported *K<sub>D</sub>*, we cannot rule out the possibility that the peptides may have some specificity, but are simply not potent. In addition, their study did not evaluate the original L5 peptide due to the reportedly poor solubility, but rather synthesized and tested the KKK-L5 to be able to use a biocompatible buffer for cell-based studies.

Nevertheless, given the unconvincing performance with regard to the specificity and potency of TJ12P1 and L5 variants in the assays, as well as their hydrophobicity, authors do not recommend further developing the current form of either peptide as a molecular imaging agent.

## Conclusions

The overexpression of GPC3 in HCC represents an opportunity to develop new imaging and therapeutic drugs for this disease, and a number of groups are working toward this goal. In this study, we assessed the GPC3 binding performance of variants of two published peptides, TJ12P1 and L5,

with purported specificity to GPC3. At concentrations in the range of the reported *K<sub>D</sub>*, the peptides demonstrate equivalent binding to GPC3<sup>+</sup> cells and GPC3<sup>-</sup> cells, and lower binding to all cell lines when compared with nonspecific peptide controls. Furthermore, in cell-free, label-free assays, neither peptide exhibited characteristics suggestive of specificity to GPC3 at submicromolar concentrations. Coupled with poor solubility in aqueous solutions and lack of demonstrable specificity and potency of TJ12P1 and L5 for GPC3, we conclude that neither is appropriate for development as molecular imaging agents.

## Acknowledgments

Authors thank Drs. Grzegorz Piszczek and Di Wu of the NHLBI Biophysics Core for assistance provided.

## Author Contributions

Conceived and designed the experiments: R.M.B., R.N., R.E.S., and F.E.E. Performed the experiments: R.M.B., O.J.K., and N.T.G. Analyzed the data: R.M.B. Wrote the article: R.M.B., O.J.K., N.T.G., R.N., R.E.S., and F.E.E. Conceptual advice given by R.N., R.E.S., Y.F., J.H., M.H., and P.L.C. All coauthors have reviewed and approved of the article before submission.

## Funding Information

This research was supported by the Intramural Research Program of the NIH, NCI, Center for Cancer Research (ZIA BC 011800; ZIA BC 010891). O.J.K. was funded by PerkinElmer, Inc. as an adjunct.

## Disclosure Statement

There are no existing financial conflicts.

**Supplementary Material**

Supplementary Data  
Supplementary Table S1  
Supplementary Figure S1  
Supplementary Figure S2  
Supplementary Figure S3  
Supplementary Figure S4

**References**

1. Llovet JM, Zucman-Rossi J, Pikarsky E, et al. Hepatocellular carcinoma. *Nat Rev Dis Primers* 2016;2:16018.
2. Forner A, Reig M, Bruix J. Hepatocellular carcinoma. *Lancet* 2018;391:1301.
3. Global Burden of Disease Cancer Collaboration, Fitzmaurice C, Allen C, et al. Global, regional, and national cancer incidence, mortality, years of life lost, years lived with disability, and disability-adjusted life-years for 32 cancer groups, 1990 to 2015: A systematic analysis for the global burden of disease study. *JAMA Oncol* 2017;3:524.
4. Marrero JA, Kulik LM, Sirlin CB, et al. Diagnosis, staging, and management of hepatocellular carcinoma: 2018 Practice guidance by the American Association for the study of liver diseases. *Hepatology* 2018;68:723.
5. Llovet JM, Ricci S, Mazzaferro V, et al. Sorafenib in advanced hepatocellular carcinoma. *N Engl J Med* 2008;359:378.
6. Kudo M, Finn RS, Qin S, et al. Lenvatinib versus sorafenib in first-line treatment of patients with unresectable hepatocellular carcinoma: A randomised phase 3 non-inferiority trial. *Lancet* 2018;391:1163.
7. Wang HL, Anatelli F, Zhai QJ, et al. Glypican-3 as a useful diagnostic marker that distinguishes hepatocellular carcinoma from benign hepatocellular mass lesions. *Arch Pathol Lab Med* 2008;132:1723.
8. Feng M, Ho M. Glypican-3 antibodies: A new therapeutic target for liver cancer. *FEBS Lett* 2014;588:377.
9. Zhu D, Qin Y, Wang J, et al. Novel glypican-3-binding peptide for in vivo hepatocellular carcinoma fluorescent imaging. *Bioconjug Chem* 2016;27:831.
10. Lee YL, Ahn BC, Lee Y, et al. Targeting of hepatocellular carcinoma with glypican-3-targeting peptide ligand. *J Pept Sci* 2011;17:763.
11. Wang Z, Han YJ, Huang S, et al. Imaging the expression of glypican-3 in hepatocellular carcinoma by PET. *Amino Acids* 2018;50:309.
12. Phung Y, Gao W, Man YG, et al. High-affinity monoclonal antibodies to cell surface tumor antigen glypican-3 generated through a combination of peptide immunization and flow cytometry screening. *MAbs* 2012;4:592.
13. Sham JG, Kievit FM, Grierson JR, et al. Glypican-3-targeting F(ab')<sub>2</sub> for 89Zr PET of hepatocellular carcinoma. *J Nucl Med* 2014;55:2032.
14. Zhang Q, Han Z, Tao J, et al. An innovative peptide with high affinity to GPC3 for hepatocellular carcinoma diagnosis. *Biomater Sci* 2018;7:159.
15. Qin Z, Wang J, Wang Y, et al. Identification of a glypican-3-binding peptide for in vivo non-invasive human hepatocellular carcinoma detection. *Macromol Biosci* 2017;17 [Epub ahead of print]; DOI: 10.1002/mabi.201600335.
16. Ishiguro T, Sugimoto M, Kinoshita Y, et al. Anti-glypican 3 antibody as a potential antitumor agent for human liver cancer. *Cancer Res* 2008;68:9832.
17. Gao W, Kim H, Feng M, et al. Inactivation of Wnt signaling by a human antibody that recognizes the heparan sulfate chains of glypican-3 for liver cancer therapy. *Hepatology* 2014;60:576.
18. Jacobson O, Weiss ID, Szajek LP, et al. PET imaging of CXCR4 using copper-64 labeled peptide antagonist. *Theranostics* 2011;1:251.
19. Quinn T, Zhang X, Miao Y. Targeted melanoma imaging and therapy with radiolabeled alpha-melanocyte stimulating hormone peptide analogues. *G Ital Dermatol Venereol* 2010;145:245.
20. Sun X, Li Y, Liu T, et al. Peptide-based imaging agents for cancer detection. *Adv Drug Deliv Rev* 2017;110–111:38.
21. Velikyan I, Haack T, Bossart M, et al. First-in-class positron emission tomography tracer for the glucagon receptor. *EJNMMI Res* 2019;9:17.
22. Zhao ZQ, Ji S, Li XY, et al. (68)Ga-labeled dimeric and trimeric cyclic RGD peptides as potential PET radiotracers for imaging gliomas. *Appl Radiat Isot* 2019;148:168.
23. Han HH, Qiu YJ, Shi YY, et al. Glypican-3-targeted precision diagnosis of hepatocellular carcinoma on clinical sections with a supramolecular 2D imaging probe. *Theranostics* 2018;8:3268.
24. Galvao J, Davis B, Tilley M, et al. Unexpected low-dose toxicity of the universal solvent DMSO. *FASEB J* 2014;28:1317.
25. Chen K, Wu Z, Zang M, et al. Immunization with glypican-3 nanovaccine containing TLR7 agonist prevents the development of carcinogen-induced precancerous hepatic lesions to cancer in a murine model. *Am J Transl Res* 2018;10:1736.
26. Li W, Xiao X, Li X, et al. Detecting GPC3-expressing hepatocellular carcinoma with L5 peptide-guided pretargeting approach: in vitro and in vivo MR imaging experiments. *Contrast Media Mol Imaging* 2018;2018:9169072.
27. Bakhshinejad B, Zade HM, Shekarabi HS, Neman S. Phage display biopanning and isolation of target-unrelated peptides: In search of nonspecific binders hidden in a combinatorial library. *Amino Acids* 2016;48:2699.